Proc. Natl. Acad. Sci. USA
Vol. 93, pp. 11179–11184, October 1996
Neurobiology

Structural recovery in lesioned adult mammalian spinal cord by x-irradiation of the lesion site

(axotomized corticospinal neurons/corticospinal tract regeneration/cavitation)

NURIT KALDERON*† AND ZVI FUKS‡

*The Rockefeller University, 1230 York Avenue, New York, NY 10021; and ‡Department of Radiation Oncology, Memorial Sloan–Kettering Cancer Center, 1275 York Avenue, New York, NY 10021

Communicated by Philip Siekevitz, The Rockefeller University, New York, NY, June 7, 1996 (received for review February 21, 1996)

ABSTRACT **Mechanical injury to the adult mammalian spinal cord results in permanent morphological disintegration including severance/laceration of brain-cord axons at the lesion site. We report here that some of the structural consequences of injury can be averted by altering the cellular components of the lesion site with x-irradiation. We observed that localized irradiation of the unilaterally transected adult rat spinal cord when delivered during a defined time-window (third week) postinjury prevented cavitation, enabled establishment of structural integrity, and resulted in regrowth of severed corticospinal axons through the lesion site and into the distal stump. In addition, we examined the natural course of degeneration and cavitation at the site of lesion with time after injury, noting that through the third week postinjury recovery processes are in progress and only at the fourth week do the destructive processes take over. Our data suggest that the adult mammalian spinal cord has innate mechanisms required for recovery from injury and that timed intervention in certain cellular events by x-irradiation prevents the onset of degeneration and thus enables structural regenerative processes to proceed unhindered. We postulate that a radiation-sensitive subgroup of cells triggers the delayed degenerative processes. The identity of these intrusive cells and the mechanisms for triggering tissue degeneration are still unknown.**

Mechanical injury to the adult mammalian spinal cord results in permanent disruption of the cord continuity and in morphological disintegration at the lesion site (1–3). This physical disruption and the apparent lack of structural recovery are due to the long-lasting degenerative processes that seem to be triggered around the site of lesion (3, 4). The cellular components that trigger these degenerative sequelae are still unknown.

Manipulation of the cellular environment by x-irradiation provides an excellent insight into the specific role of individual cell types within the tissue under normal and pathological conditions. X-irradiation has been used to determine patterns of cytogenesis and morphogenesis in developing mammalian central nervous system (CNS) (e.g., see refs. 5 and 6). A localized and timed x-irradiation during CNS morphogenesis also enabled the selective removal of the glia limitans and the demonstration of its role as a protective layer of the CNS from invading "foreign" cells (7).

We have used x-irradiation as a tool for selective removal of reactive cells generated in response to CNS injury, thus demonstrating that the pathological consequences in lesioned adult rat olfactory bulb can be averted (8). We found in the severed olfactory bulb that irradiation delivered within a defined time-window, 2–3 weeks postinjury (PI), substantially altered the cellular composition around the site of incision; formation of reactive astrocytes and concomitantly the degenerative structural consequences of injury were abolished, including the cavitation and death of the axotomized principal neurons which were prevented (8).

Here, our objective was to examine whether irradiation treatment, which elicited beneficial effects in the lesioned olfactory bulb (8), would facilitate in sectioned adult rat spinal cord recovery processes, specifically, the restitution of structural continuity and the regrowth of severed corticospinal (CS) axons into the distal stump. For this purpose, the lesion consisted of a complete transection of the left side (hemisection) extending always over into the right side of the spinal cord at low thoracic level (Fig. 1). This injury resulted in localized degeneration and cavitation around the site of incision and in complete severance of the left and right CS axonal tracts (9, 10). Analysis for recovery was performed exclusively on the left hemicord and on the left CS tract. Morphological recovery was determined by histological analysis of each of the lesion sites; this analysis was performed on serial longitudinal sections of the cords using the central canal as a natural marker delineating the border between the two sides (Fig. 1). Regeneration of the severed CS axons into the distal stump was examined by axonal dye transport—i.e., quantitatively by retrograde double-labeling of the CS neurons and qualitatively by anterograde tracing of the CS axons. In addition, we examined the natural course of degeneration and cavitation at the site of lesion with time after injury. Short accounts of this study have appeared in abstract forms (11–13).

METHODS

Injury. Adult Sprague–Dawley female rats (Charles River Breeding Laboratories), 3–6 months old, were anesthetized with 7% chloral hydrate injected i.p. (0.6 ml per 100 g of body weight), and with Stadol (butorphanol) injected s.c. (0.02 mg per 100 g of body weight). Under aseptic conditions, the spinal cord was exposed by laminectomy at vertebral level T12 and then by slitting the overlying menninges. The entire left hemicord at T12–T13 was transected, first with a microblade and then with microscissors, cutting also the lateral and ventral menninges but avoiding the posterior artery; the incision always extended half-way into the right side of the cord (Fig. 1). In certain experiments (as indicated), after cutting the cord the suture–loop procedure was performed. A loop was made with a suture around the cord tissue which remained intact, and the loop-enclosed tissue was cut with scissors. To create a loop around the tissue, the surgical microneedle attached to the suture #8-0 was threaded from left to right underneath the

The publication costs of this article were defrayed in part by page charge payment. This article must therefore be hereby marked "*advertisement*" in accordance with 18 U.S.C. §1734 solely to indicate this fact.

Abbreviations: CS, corticospinal; CNS, central nervous system; DL–CS, double-labeled CS; FB, fast blue; HRP, horse-radish peroxidase; PI, postinjury; diI, 1,1′-dioctadecyl-3,3,3′,3′-tetramethylindocarbocyanine perchlorate.

†To whom reprint requests should be sent at the present address: Memorial Sloan–Kettering Cancer Center, Box 280, 1275 York Avenue, New York, NY 10021. e-mail: kalderon@mskcc.org.

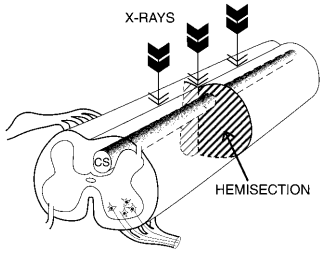

FIG. 1. Experimental paradigm. Approaching from the left, about ¾ of the cord was cut at T12–T13; therefore the left side of the cord was completely cut (hemisection). In the rat, the crossed CS tracts descend in the dorsal funiculus (9), and the CS tracts are completely crossed below midthoracic level (10). Thus, this hemisection severed the entire left CS tract. X-irradiation was centered around the lesion site. For histology, a piece of the cord containing the incision site was serially sectioned in a longitudinal plane.

dorsal artery and inserted into the center of the right side of the cord, then pushed straight down toward the bottom of the spinal cavity, and then laterally and up surrounding with the suture the entire left side and part of the right side of the cord. Upon completion of the injury, the site of incision was covered with a piece of Durafilm (Codman & Shurtleff, Randolph, MA) (14), and the cavity created due to the laminectomy was filled with Gelfoam (Upjohn). The overlying back muscles were sutured, the skin was closed with surgical wound clips, and the rat was given a s.c. injection of long-acting penicillin (300,000 units). When needed, bladders were expressed manually until their automatic function was resumed.

Radiation. Irradiation was delivered by an x-ray generator, a hybrid orthovoltage unit operating at 320 kVp, 10 mA with 0.5 mm Cu filtration, at a dose rate 149 cGy/min, at a distance of 50 cm from the skin. Treatment was delivered through a posterior approach (Fig. 1) while the rat is anaesthetized and shielded with lead except for the exposed treatment field, the dimensions of which were 25 mm × 20 mm (length × width).

Histology. Anaesthetized rats were perfused with a phosphate-buffered saline solution and then with a solution of 6% formaldehyde in phosphate-buffered saline (8). After removal from the vertebrae and the skull, appropriate tissue samples were further fixed and frozen (15). Frozen cord samples were cryostat-sectioned in a longitudinal plane; the serially collected sections were kept at −20°C until processed. For routine analysis cord sections (15–20 μm thick) were stained with thionin and examined by light microscope.

Retrograde Double-Labeling of CS Neurons. Two different dyes were applied at distinct times PI for the differential labeling in the motor cortex of axotomized and regenerated CS neurons. First, to label the axotomized CS neurons by retrograde axonal transport, we applied at the time of injury into the cut 1,1′-dioctadecyl-3,3,3′,3′-tetramethylindocarbocyanine perchlorate (diI) (red), which labels the plasma membrane (16) and is long lasting (17). Second, to label the CS neurons whose axons regenerated to a certain region distal to the initial cut, we applied after the recovery period into that region in the distal stump fast blue (FB) (blue), which labels the cytoplasm (18). Immediately following injury a pledget of Gelfoam soaked with 2.5 μl of 0.3% diI (Molecular Probes) suspension in 0.15 M NaCl and 2% Triton X-100 (17) was inserted into the site of lesion for 15–20 min. Two to 3 months after injury, the distal cord (L3–L5) was exposed by laminectomy. A 1% aqueous solution of FB (Sigma) was injected into the left hemicord, in 5–6 lateral spots, at a distance of 8–10 mm distal to the lesion site; a total of 1.5 μl FB was injected per spinal cord, and 4 days later the cord and brain were fixed and processed for analysis. Since in the rat the left CS tract is completely crossed below midthoracic level (10), the analysis to determine its regrowth was performed only in the right brain

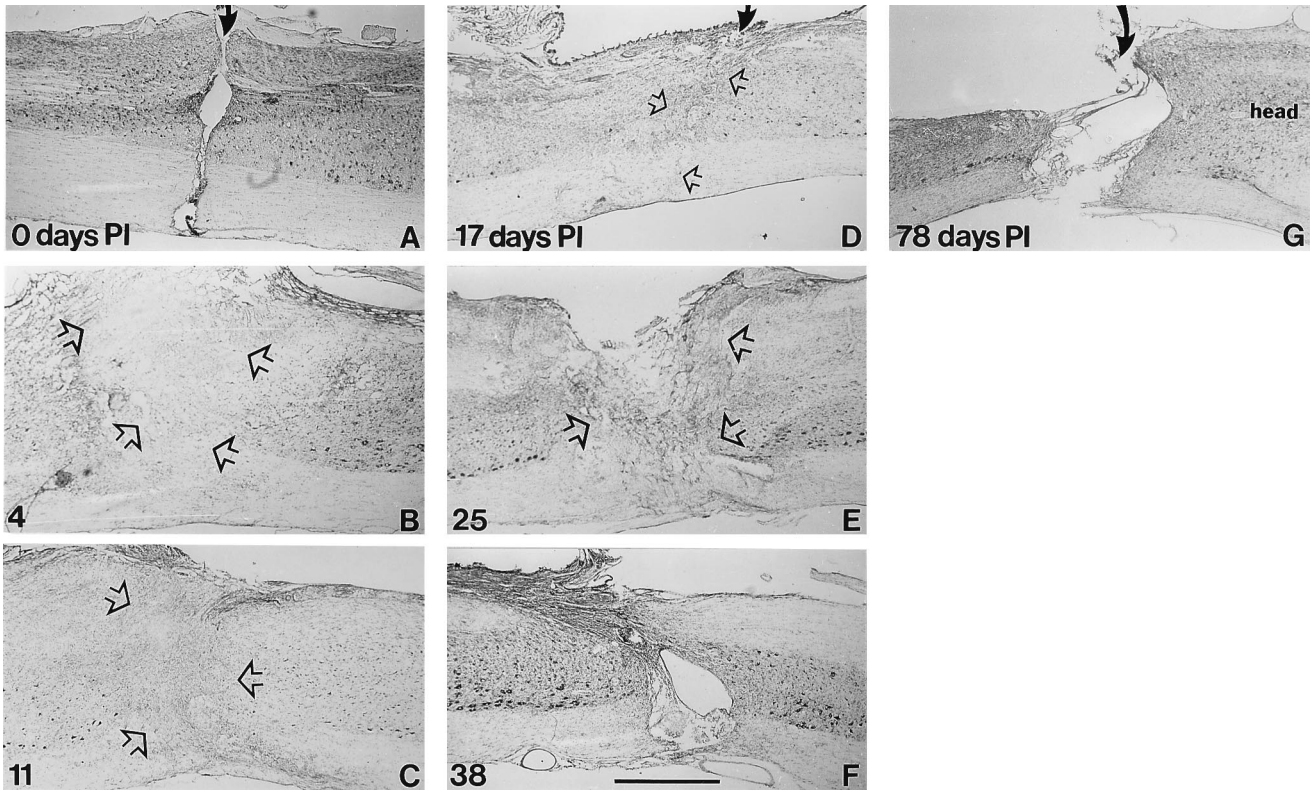

FIG. 2. Temporal consequences of transection—intrinsic morphological features at the site of incision of untreated cords (*A–G*) at days 0, 4, 11, 17, 25, 38, and 78 PI. Micrographs of thionin-stained sagittal sections through lesioned cords (taken at 0.75–0.9 mm from the lateral edge). Indicated are the site of incision (arrows) and the edges of the cord stumps (clear arrows). Note that by day 11 PI (*C*) the two stumps seem to be reconnected while the first signs of degeneration are detected by day 25 PI (*E*). (Bar = 1 mm.)

hemisphere. The right brain hemisphere was sagittally cryostat-sectioned (25 μm thick); sections were coverslipped with 50% glycerol in phosphate-buffered saline and examined with a Zeiss microscope equipped with epi-illumination optics with an exciter-barrier filter combination for fluorescent dyes.

Anterograde Labeling of CS Axons. The tracer, horse-radish peroxidase (HRP), was injected into the motor cortex; labeled CS axons were visualized in cord sections in regions around and distal to the cut. Two to 3 months PI, the dorsal surface of the right hemicortex of anaesthetized rats was exposed by a craniotomy. A total of 1.6 μl (per cortex) of 30% HRP (Boeringher Mannheim) was injected into 6–7 separate spots aligned parallel to the midline, from bregma anterior-posterior +1 to −4 mm, at 2 mm from the midline. Two days later rats were fixed and the cords were collected, frozen, and horizontally sectioned (30 μm thick). Animal fixation and processing of the slide-mounted sections for HRP histochemistry with tetramethyl benzidine as substrate were performed (19). HRP labeled axons were visualized under dark-field illumination microscopy. Since this method cannot distinguish between severed and intact axons, the cord injury in this experiment included the suture–loop procedure, which assures complete severing of the left CS tract.

RESULTS

The Critical Time-Window for Preventing Tissue Degeneration. The end result of transection of the spinal cord is a morphological disintegration at the lesion site and a large cavitation (Fig. 2*G*). Histological examination of the time course of the sequelae of lesion (Fig. 2) suggests that the onset of the degenerative processes occurs sometime at the end of the third week PI. Initially, a normal course of wound healing events was observed similar to that seen in most nonneural tissues. At the first few days PI, the two cord stumps appeared to be swollen and separated by a gap (Fig. 2*B*); then the gap vanished and the stumps appeared to be connected (Fig. 2*C*), and later, at days 17–19 PI, the cord seemed to be fused with very little signs of the initial cut (Fig. 2*D*). The decay processes were first noticeable during the fourth week PI as discrete sites of tissue disintegration (Fig. 2*E*); these presumably propagated at later periods (second month PI) resulting in two cord stumps separated by a large cavity (in the millimeter range) (Fig. 2 *F* and *G*). Innate structural recovery events during the second and third week PI similar to those described here were previously observed in a crushed rat spinal cord (20).

The effectiveness of the timing of radiation in preventing tissue degeneration in the lesioned spinal cord was examined in treated and untreated cords at 60 days PI. We selected a radiation dose and time points based on data obtained previously in the lesioned olfactory bulb (8). The lesioned cords were irradiated with a single dose of 10 Gy at the first, second, third, and fourth week PI (n = 24), and were compared with unirradiated lesioned cords (n = 8). Irradiation within this period (6–31 days PI) seemed to attenuate the decay process (Fig. 3), as the normally occurring cavitation (e.g., Fig. 2*F*) was not manifested as yet. Radiation was effective in preventing tissue degeneration when applied within the third week PI; its maximal effect was exerted when applied at days 17–18 PI (Fig. 3*B*). In this optimal range, degeneration was confined to a few small pockets and the gap between the cord stumps was minimal (a few cells' size). Radiation delivered either before (Fig. 3*A*) or beyond the third week PI (Fig. 3*C*) was ineffective in preventing the structural decay or in decreasing its size (in the millimeter range). In addition, we examined for gliosis in the above samples and found that timed irradiation reduced/eliminated reactive astrocytes in the lesioned cord in a similar manner to that found in the lesioned olfactory bulb (8)—i.e., optimal timing during the third week PI. Thus, it appears that the two periods, the period in which transient structural recovery is observed (Fig. 2*D*) and the period in which irradiation can prevent gliosis and tissue degeneration (Fig. 3*B*), are identical.

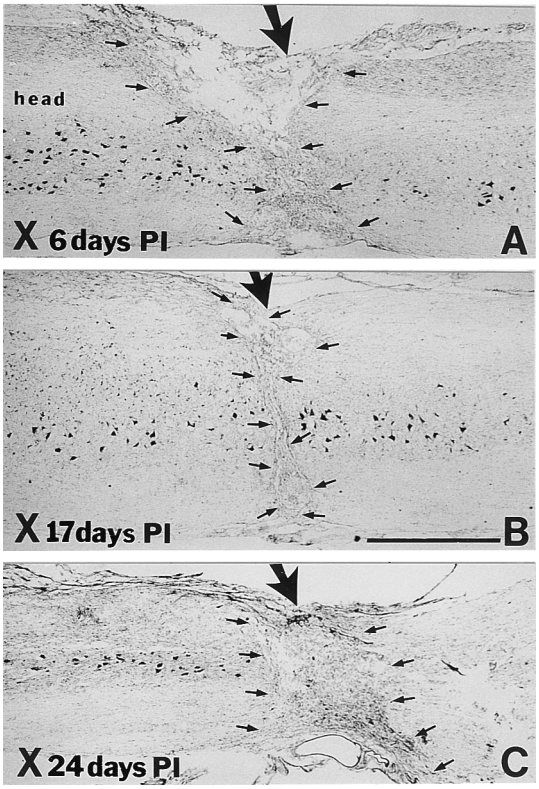

FIG. 3. The critical time-window for preventing tissue degeneration. Morphology of the lesion sites (arrow) in thionin-stained sagittal sections through three lesioned cords which were irradiated at days 6 (*A*), 17 (*B*), and 24 (*C*) PI. Tissue disintegration seen between the edges of the two stumps (small arrows) is extensive in the lesioned cords treated on days 6 and 24 PI; in contrast, it is minimal in the cord irradiated on day 17 PI. (Bar = 1 mm.)

Irradiation Restitutes Permanent Structural Continuity. We next examined the effectiveness of radiation in preventing the degenerative processes when delivered under optimal conditions. The lesioned cords were irradiated on days 17–18 PI with a single dose of 20 Gy, which is within the optimal dose range (17–23 Gy) for eliciting structural recovery in the olfactory bulb (8). In all treated cords (n = 31), degeneration and cavitation were prevented to a variable degree as compared with untreated cords (n = 26); in some (n = 4), a marked structural continuity was established as illustrated in Fig. 4. For comparison, in the control unirradiated lesioned cord a continuous cavity of up to 1 mm in width occupied most of the left hemicord (Fig. 4 *B–E* and *DD*). In contrast to the control, in the irradiated lesioned cord there was partial preservation of tissue morphology, cavitation was diminished (Fig. 4 *Ax–Ex* and *DDx*), and structural continuity was established. In this treated cord, within a large portion (40%) of its left side structural continuity was established (Fig. 4 *Bx–Ex*), and, as shown in the next section, about a third of its severed CS axons regrew back to their general projection field, 9 mm distal to the cut.

Regeneration of Severed CS Axons Beyond the Lesion Site. Following x-ray therapy of the lesion site, some of the severed CS axons regrew across the lesion site and into the distal stump as was determined using retrograde and anterograde axonal dye-transfer procedures. The degree of regrowth 8–10 mm past the lesion site of the severed CS axons in irradiated (n = 23) and control untreated (n = 8) rats was determined by the retrograde double-labeling procedure. Treated lesioned cords

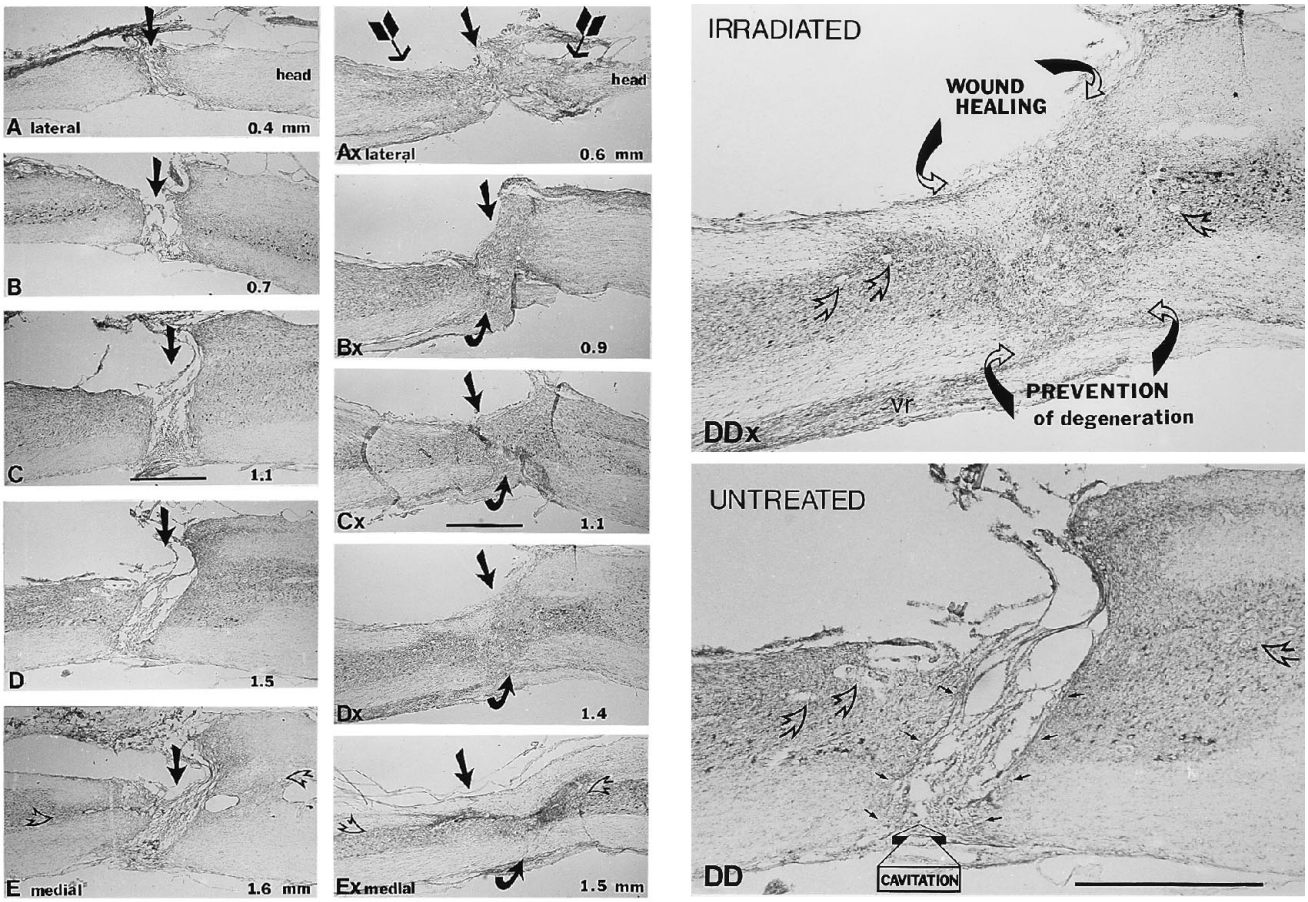

FIG. 4. Restitution of structural continuity. A serial reconstruction of the site of lesion of two transected hemicords, one untreated (*A–E*) and one irradiated 18 days PI (*Ax–Ex*) analyzed at 78 days PI and 86 days PI, respectively. (*A–E* and *Ax–Ex*). Composites of thionin-stained sagittal sections taken from regions situated at different distances (mm) from the lateral edge of each of the hemicords. (*DDx* and *DD*). High magnification micrographs of the lesion site in an irradiated and a control cord-sections seen in *Dx* and *D*, respectively. Indicated are entry (straight arrows) and exit (curved arrows) of incision, the central canal (clear arrowheads), and a ventral root (vr). In the untreated cord, the stumps with a scar tissue at their edges (small arrows) are separated by a cavity filled with extracellular matrix (*DD*); this cavity extends throughout the entire volume of the injured hemicord (*A–E*). In contrast, in the irradiated cord (tailed arrows) tissue decay was prevented and structural continuity was established (*DDx*) within a large portion of the lesioned hemicord (*Cx–Ex*). (Bars = 1 mm.)

received a single dose of either 15, 17.5, 18.5, or 20 Gy at 18 days PI; selection for treatment and type of treatment was randomized. The total number of double-labeled CS (DL–CS) neurons (Fig. 5 *A* and *B*) in the right cortex of each of the rats were counted, and the corresponding individual sums were plotted in Fig. 5*C*. (This counting was performed on alternate sections to avoid counting the same cell twice thus yielding approximately half the actual sum.) In addition, the total numbers of the CS neurons projecting normally to and/or passing the sites of application of the first (T12–T13) and second dye (L3–L5) were determined in normal intact rats by retrograde labeling; these sums are 1600 and 600, respectively, and are in good agreement with comparable numbers in the literature (21). The estimated values of the degree of recovery, i.e., degree of regrowth of the severed CS axons to L3–L5 region, were expressed as percentage of DL–CS out of 600.

A marked increase in the sums of DL–CS neurons was observed in a third of the rats irradiated with 17.5–20 Gy as compared with the control group (Fig. 5*C*), showing that these rats had ''good'' recovery values—i.e., 20–59% of the axotomized CS neurons regrew their axons back to their general target field. Very few DL–CS neurons (12 ± 10) were found in control rats whose lesioned cords were not irradiated; this amounts to a mean recovery value of 2 ± 1.67%, which statistically is not different from a zero recovery. Irradiation with 15 Gy did not result in a change in the number of DL–CS neurons (7 ± 6) or in mean recovery value (1.16 ± 1.05%) as compared with the control group. In contrast, in the 17 rats treated with 17.5–20 Gy statistical paired comparisons test for change in recovery values shows that this treatment resulted in effective recovery of the severed CS axons as compared with the control group; the group's mean difference in recovery values is 10.9 ± 4.8% (*t* test, $P < 0.01$). Further analysis of these rats shows that 8 of 17 did not have any recovery and that 7 of 17 had a mean recovery value of 27.6 ± 16.3% which is significantly ($P < 0.005$) different from the mean value in the control group. Finally, a correlation was found between axonal recovery as measured by the sums of DL–CS neurons and the restoration of structural continuity at site of incision. For example, the rats whose cords are seen in Fig. 4 were also analyzed for axonal regeneration; the irradiated rat (Fig. 4 *Ax–Ex*) had 205 DL–CS neurons (34.16% recovery) compared with only 22 DL–CS neurons found in the untreated rat (Fig. 4 *A–E*)—i.e., a 9.3-fold increase in the treated rat.

The following additional observations suggest that the first retrograde-labeling was specific due to axotomy, and that the second labeling was specific and due to regrowth of the severed axons into the distal stump and not due to diffusion of the dye. First, no cells were found within the cortex that were only labeled with the second dye. Secondly, the diI-labeled neurons in the motor cortex (e.g., Fig. 5*A*) were found to be restricted topologically within a longitudinal band whose location and size fits well with the reported topology of the CS neurons projecting to the lumbosacral cord (22, 23). This band was

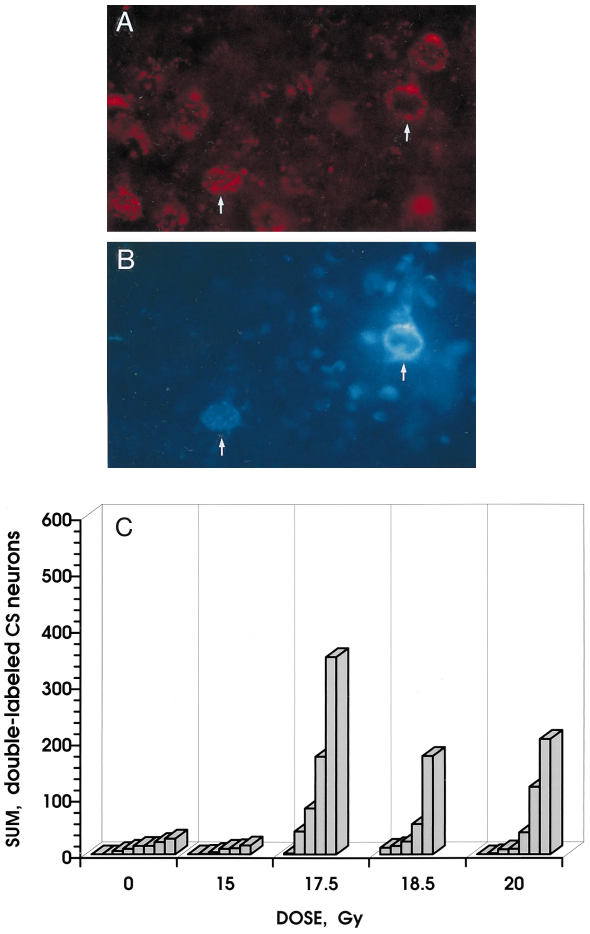

FIG. 5. Degree of recovery of axotomized CS neurons—retrograde double-labeling. Micrographs of a cortical section (*A* and *B*) taken from rat with lesioned and irradiated cord; this section was photographed for diI labeling (red) (*A*) and for FB labeling (blue) (*B*). Seen in this section are 11 diI-labeled CS cells (i.e., axotomized) (*A*) but only 2 of them (arrows) are double-labeled; these 2 cells (in *B*) are also labeled by FB (arrows) (i.e., regrown axons 10 mm into the distal stump). Note the FB-labeled dendrites surrounding the neuron on the right (*B*). (*C*) The individual sums of the DL–CS neurons in each of the rats (bars) with lesioned cords which were untreated ($n = 8$) and treated ($n = 23$) with different doses of x-rays are plotted. Our measured number of 600 CS neurons projecting normally to the application site of FB was used as the maximal expected sum of DL–CS neurons. Cord injury in the 18.5-Gy-treated group included also the suture–loop procedure, and two rats of the 15-Gy-treated group were analyzed at 41 days PI. Note the increase in the sums of DL–CS in the groups treated with 17.5–20 Gy.

≈2-2.2 mm wide and aligned in parallel to the midline at 0.8–1.0 mm from it. Furthermore, within this band a large portion of the DL–CS neurons (Fig. 5 *A* and *B*) were located caudally and closer to the midline, at sites projecting to the sacral cord (22). Finally, it was found in all cords that FB diffused up to 2 mm from its injection site—i.e., 6–8 mm away from the lesion site.

Data obtained with the axonal tracing method (Fig. 6) confirm and are consistent with those obtained with the neuronal labeling procedure. These data suggest that when structural continuity was established, the majority of the severed CS axons regenerated into the distal stump and terminated their regrowth at L1–L2 (lumbar enlargement), while only a small portion extended all the way to the sacral cord. The pattern and extent of regrowth of the severed CS axons beyond the lesion site were examined in irradiated ($n = 9$) and control ($n = 8$) lesioned cords 2–3 months PI. Radiation (20 Gy) was delivered at 17–18 days PI, and selection for

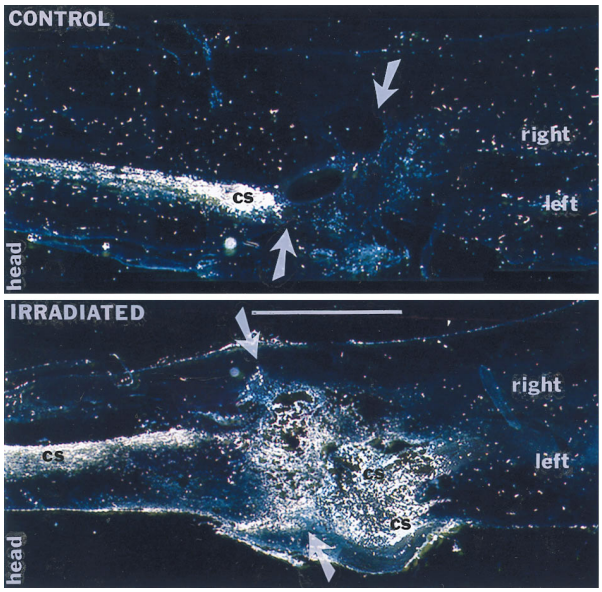

FIG. 6. The terrain of regrowth of severed CS tract. Dark-field micrographs of horizontal cord sections in which the HRP-labeled CS axons are depicted as bright-yellowish granular strings; however, due to the low-magnification, an individual axon cannot be discerned here (here, the tract contains ≈3000 axons). Sections were taken 90 days PI from an untreated cord (*Upper*) and an irradiated cord (*Lower*). Images were computer-generated by combining from different tissue sections the areas around the lesion site which contained high density of labeled axons. These areas were condensed into a single two-dimensional section, thus showing the majority of the severed CS axons and their terrain of regrowth. In both cords, anterior to the cut (arrows) only the left CS tract (cs) is labeled, seen as a white ribbon on a dark background. In the control cord (*Upper*) the CS axons did not cross the lesion site (arrows) and are found in front of the cavity. In the treated cord (*Lower*) structural continuity was established and the severed CS axons (cs) crossed the lesion site (arrows) and grew bilaterally ≈2.5 mm into the distal stump covering there an extensive area. (Bar = 2 mm.)

treatment was randomized. The severed CS axons regrew across the lesion site and extended into the distal portion of the cord (Fig. 6 *Lower*) in those irradiated lesioned cords in which a marked structural continuity was obtained ($n = 4$). It appears that a large portion of the severed CS axons crossed the lesion site and regrew for at least 2–3 mm deep into the distal stump; however, these were no longer confined to a discrete tract location (Fig. 6 *Lower*). The regenerated CS axons extended bilaterally into the white matter; they also grew into the grey matter and terminated there, and some reached distances of at least 12 mm distal to the cut (data not shown). In contrast to the irradiated cords, in the untreated lesioned cords the severed CS axons did not cross the lesion site and remained at the edge of the cavity anterior to the cut (Fig. 6 *Upper*).

In evaluating the potential beneficial effects of irradiation, one should bear in mind that the distortions in the pattern of axonal regrowth are due in part to the experimental conditions which were designed to assure severance leading to misalignment of the cord stumps. It is assumed that upon proper alignment of the cord stumps the severed axonal fibers will have a better opportunity to reinnervate their target fields. Further, the incidence of an "excellent" structural recovery as seen in Fig. 4 is ≈11.5% (7/61). It is assumed that enhancing the extent of structural recovery would be followed by an increase in incidence and degree of recovery of the severed CS tract. Preliminary data show that the variability in the degree of structural recovery is related in part to the closing of the wound. The incidence and degree of structural recovery are increased when the pressure on the tissue is reduced.

DISCUSSION

This study shows that irradiation can substantially alter the cellular response and sequelae after injury in lesioned adult mammalian spinal cord, and that this capacity is time-dependent. It shows that appropriate irradiation leads to restitution of structural continuity. Data described here and in an accompanying paper (24) suggest that prevention of tissue degeneration and establishment of structural continuity are a sufficient requirement for the severed CS axonal tracts to regrow, traverse the lesion site, extend deep into the distal stump, and reestablish synaptic connectivity with neurons within the target field in the distal cord stump.

Several conclusions can be inferred from the data presented here; some of these conclusions are also supported by observations published by us and others. First, the adult mammalian spinal cord appears to have innate mechanisms necessary for recovery from mechanical injury (1, 4, 20). Second, a distinctive feature of the spinal cord is the existence of a latent degenerative pathway which is triggered after recovery processes are already in progress. Third, this degenerative pathway can be suppressed by x-irradiation and the intrinsic recovery repertoire can proceed unhindered (8). Fourth, timing of the treatment after the injury is a most crucial factor in overcoming the degenerative process; in the rat, it is during the third week after injury.

The phenomena of initial regeneration and delayed degeneration were described by Ramón y Cajal as abortive regeneration (1). He noted that at first there is a constructive process in the severed fiber tracts of injured spinal cord, and that the degenerative response in the regrowing axons is triggered only by the third week after injury. A similar time-course on the molecular level was observed in axotomized rubrospinal neurons in which mRNA levels of proteins required for axonal regrowth were elevated during the first week and were reduced only by the second week after axotomy (25). Presumably, axonal regeneration is halted by the ensuing tissue degeneration.

The cellular events that trigger tissue degeneration and cavitation in injured CNS are still unknown, even though it has been known for almost a century that these are related to the degree of damage caused to the vascular system—i.e., cavitation is minimal when the cut is in parallel to the blood vessels (1). Our observations that the degenerative response can be permanently prevented by timed irradiation imply that cells that are eradicated by irradiation are those which trigger the degenerative pathway. Our data in the olfactory bulb (8) and here show a correlation between the prevention of degeneration and of cavitation and the elimination/prevention of gliosis. These suggest that glial scarring may play a primary role in initiation of the degenerative responses—e.g., by preventing appropriate revascularization (26) it would be inducing necrosis. At present our study does not identify which of the cell types—e.g., microglia/macrophages, astrocytes—are directly affected by the irradiation or which of these are involved in initiating tissue degeneration. Regardless of the mechanism, our findings provide sufficient grounds for developing x-irradiation into a posttraumatic therapeutic procedure for facilitating the innate constructive processes in injured spinal cord.

This paper is dedicated to the late Alex Mauro whose scientific enthusiasm, intellectual support, and unfailing encouragement provided the only resources to pursue this research. N.K. is indebted and grateful to Joshua Lederberg, Jerome Posner, and Torsten Wiesel for devoting their time to helpful and critical discussions of the data and experimental design during the course of this study. We are thankful to Jim Palmer who participated in the early phases of the study for excellent technical assistant, and to Mimi Halpern and Patricia Wade for their comments and suggestions in reading earlier versions of the paper.

1. Ramón y Cajal, S. (1928) *Degeneration and Regeneration of the Nervous System*, trans. May, R. M. (Oxford Univ. Press, London), Vol. 2, pp. 482–713.
2. Noble, L. J. & Wrathall, J. R. (1985) *Exp. Neurol.* **88,** 108–122.
3. Kakulas, B. A. (1987) *Paraplegia* **25,** 212–216.
4. Bresnahan, J. C. (1978) *J. Neurol. Sci.* **37,** 59–82.
5. Gilmore, S. A. (1966) *Neurology* **16,** 749–753.
6. Altman, J. & Anderson, W. J. (1972) *J. Comp. Neurol.* **146,** 355–406.
7. Blakemore, W. F. & Patterson, R. C. (1975) *J. Neurocytol.* **4,** 573–585.
8. Kalderon, N., Alfieri, A. A. & Fuks Z. (1990) *Proc. Natl. Acad. Sci. USA* **87,** 10058–10062.
9. Brown, L. T. (1971) *Exp. Brain Res.* **13,** 432–450.
10. Vahlsing, H. L. & Feringa, E. R. (1980) *Exp. Neurol.* **70,** 282–287.
11. Kalderon, N., Palmer, J., Alfieri, A., Kim, J. H. & Fuks, Z. (1989) *Soc. Neurosci. Abstr.* **15,** 333.
12. Kalderon, N. & Fuks, Z. (1991) *Soc. Neurosci. Abstr.* **17,** 565.
13. Kalderon, N., Fuks, Z. & Schwartz-Giblin, S. (1993) *Soc. Neurosci. Abstr.* **19,** 681.
14. Krikorian, J. G., Guth, L. & Donati, E. J. (1981) *Exp. Neurol.* **72,** 698–707.
15. Kalderon, N. (1988) *J. Neurosci. Res.* **21,** 501–512.
16. Honig, M. G. & Hume, R. I. (1986) *J. Cell Biol.* **103,** 171–187.
17. Vidal-Sanz, M., Villegas-Pérez, M. P., Bray, G. M. & Aguayo, A. J. (1988) *Exp. Neurol.* **102,** 92–101.
18. Bentivoglio, M., Kuypers, H. G. J. M., Catsman-Berrevoets, Loewe, H. & Dann, O. (1980) *Neurosci. Lett.* **18,** 25–30.
19. Mesulam, M.-M. (1978) *J. Histochem. Cytochem.* **26,** 106–117.
20. Guth, L., Barrett, C. P., Donati, E. J., Anderson F. D., Smith, M. V. & Lifson, M. (1985) *Exp. Neurol.* **88,** 1–12.
21. Hicks, S. P. & D'Amato, C. J. (1977) *Exp. Neurol.* **56,** 410–420.
22. Ullan, J. & Artieda, J. (1981) *Neurosci. Lett.* **21,** 13–18.
23. Leong, S. K. (1983) *Brain Res.* **265,** 1–9.
24. Kalderon, N. & Fuks, Z. (1996) *Proc. Natl. Acad. Sci. USA* **93,** 11185–11190.
25. Tetzlaff, W., Alexander, S. W., Miller, F. D. & Bisby, M. A. (1991) *J. Neurosci.* **11,** 2528–2544.
26. Jiang, B., Bezhadian, M. A. & Caldwell, R. B. (1995) *Glia* **15,** 1–10.

Proc. Natl. Acad. Sci. USA
Vol. 93, pp. 11185–11190, October 1996
Neurobiology

Severed corticospinal axons recover electrophysiologic control of muscle activity after x-ray therapy in lesioned adult spinal cord

(paralysis/recovery of posture/reinnervation/restitution of function)

NURIT KALDERON*† AND ZVI FUKS‡

*The Rockefeller University, 1230 York Avenue, New York, NY 10021; and ‡Department of Radiation Oncology, Memorial Sloan–Kettering Cancer Center, 1275 York Avenue, New York, NY 10021

Communicated by Joshua Lederberg, The Rockefeller University, New York, NY, July 9, 1996 (received for review February 21, 1996)

ABSTRACT **Mechanical injury to the adult mammalian spinal cord results in permanent loss of structural integrity at the lesion site and of the brain-controlled function distal to the lesion. Some of these consequences were permanently averted by altering the cellular constituents at the lesion site with x-irradiation delivered within a critical time window after injury. We have reported in a separate article that x-irradiation of sectioned adult rat spinal cord resulted in restitution of structural continuity and regrowth of severed corticospinal axons across and deep into the distal stump. Here, we report that after x-ray therapy of the lesion site severed corticospinal axons of transected adult rat spinal cord recover electrophysiologic control of activity of hindlimb muscles innervated by motoneurons distal to the lesion. The degree of recovery of control of muscle activity was directly related to the degree of restitution of structural integrity. This restitution of electrophysiologic function implies that the regenerating corticospinal axons reestablish connectivity with neurons within the target field in the distal stump. Our data suggest that recovery of structural continuity is a sufficient condition for the axotomized corticospinal neurons to regain some of their disrupted function in cord regions distal to the lesion site.**

Mechanical injury to the adult mammalian spinal cord results in irreversible paralysis of the muscles innervated by motoneurons distal to the lesion site, and in permanent disruption of the cord continuity at the lesion site (1–3). The permanent muscle paralysis is due to the severance/laceration of descending brain–spinal cord fibers that control motoneurons' activities (1). The physical disruption and the lack of structural recovery are due to the long-lasting degenerative processes (3, 4) that seem to be triggered around the site of lesion a few weeks after the injury (5).

We demonstrated previously (5, 6) that prevention of degeneration and structural recovery can be obtained in lesioned adult mammalian central nervous system (CNS) by modifying the cellular environment at the lesion site with x-irradiation provided it was delivered within a critical time window after injury. The restitution of structural continuity by the x-ray therapy of the lesion site, in injured olfactory bulb (6) and spinal cord (5), was associated also with structural recovery in axotomized neurons and severed fiber tracts. Irradiation in the severed olfactory bulb was accompanied by a rescue of some of the axotomized mitral cells from death (6) and in the sectioned spinal cord by the regrowth of some of the severed corticospinal (CS) axons across the lesion site and deep into the distal spinal cord stump (5).

Here, our objective was to determine whether the recovery in structure which is elicited by x-ray therapy is accompanied also by recovery of some of the disrupted function of the severed CS tract. We examined, under irradiation conditions that enable structural recovery, whether the regenerating CS axons reestablish synaptic connectivity with neurons within the distal stump. We determined whether the severed CS axons recover their electrophysiologic control on muscle activity distal to the lesion. For this purpose, the experimental lesion consisted of a complete transection of the left side (hemisection) extending over into the right side of adult rat spinal cord at segmental level T12–T13. This lesion resulted in complete severance of the left and right CS axonal tracts (7, 8). In addition, in several of the experimental lesions a bilateral complete transection of the cord was performed; thereby all the brain–spinal cord fiber tracts were severed completely. Electrophysiologic recovery was examined exclusively in the left CS tract; the pertinent studies were performed in the right cortical hemisphere because the neuronal cell bodies of this tract are situated in the right motor cortex (7, 8). The hindlimb area (9–11) of the right primary motor cortex was electrically stimulated and the evoked electromyogram (EMG) responses were recorded in several left hindlimb muscles innervated by lumbar and sacral motoneurons. As internal controls, evoked EMG responses were recorded also in a left forelimb muscle (proximal to the lesion site) and in a right hindlimb muscle (not controlled by the left CS tract). Finally, the potential of eliciting recovery of function of the hindlimbs by the x-ray therapy was evaluated by a comparative visual examination of the treated versus untreated rats, both of which sustained a complete spinal cord transection.

METHODS

Spinal Cord Injury. *Hemisection.* Adult Sprague–Dawley female rats (Charles River Breeding Laboratories), 3–6 months old, were anesthetized with 7% chloral hydrate injected i.p. (0.6 ml per 100 g of body weight), and with 0.2% Stadol (butorphanol) injected s.c. (0.01 ml per 100 g of body weight). Using a dissection microscope the spinal cord was exposed by laminectomy at vertebral level T12; the entire left hemicord was transected at segmental level T12–T13, and the incision always extended half-way into the right side of the cord (5). Finally, a loop was made with a surgical suture #8-0 around the cord tissue which remained intact, and the loop-enclosed tissue was cut with microscissors (5).

Complete transection. The two sides of the cord were cut as described for hemisection. Next, a loop was made with a surgical suture #8-0 that was threaded underneath the dorsal artery and around the entire cord tissue which remained intact, and the loop-enclosed tissue was cut. Upon completion of the injury, to prevent compression of the cord by the side muscles,

The publication costs of this article were defrayed in part by page charge payment. This article must therefore be hereby marked "*advertisement*" in accordance with 18 U.S.C. §1734 solely to indicate this fact.

Abbreviations: CS, corticospinal; CNS, central nervous system; EMG, electromyogram.

†To whom reprint requests should be sent at the present address: Memorial Sloan–Kettering Cancer Center, Box 280, 1275 York Avenue, New York, NY 10021. e-mail: kalderon@mskcc.org.

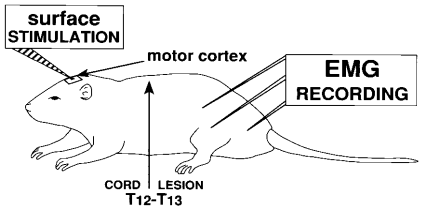

FIG. 1. Experimental paradigm: recording of CS-evoked EMG responses. The exposed surface of the right primary motor cortex of anaesthetized rat was electrically stimulated and the evoked responses were recorded in the left forelimb and hindlimb muscles and in right hindlimb muscles.

a strip of synthetic film (Durafilm; Codman & Shurtleff, Randolph, MA) was placed along each of the sides between the vertebra and the muscle and sutured at a few points to the side muscle. The overlying back muscles were sutured, the skin was closed with surgical wound clips, and the animal was given a s.c. injection of long-acting penicillin (300,000 units). When needed, bladders were expressed manually until automatic function was resumed; otherwise, no special postsurgical care was needed. At the end of the experiment, the rats were sacrificed and their cords around the lesion site were histologically examined (5).

Radiation. X-irradiation was delivered by a Clinac 600C linear accelerator (Varian) using a 6-MV beam at a dose rate of 200 cGy/min. Treatment was delivered through a posterior approach while the rat was anaesthetized, at a source-to-skin distance of 100 cm with a tissue buildup superflab of 1 cm. The dimensions of the radiation field were 25 mm × 20 mm (length × width) centered at the site of lesion. Radiation therapy was delivered as a single dose of 20 gray (Gy) at 17–18 days postinjury, and selection for treatment was randomized. At this dose level and the recovery period given until analysis was performed (2–5 months postinjury), no side effects were noticed except for hair loss limited to the radiation exposed field only.

Electrophysiology. EMG recordings were performed on pentobarbital anaesthetized rats clamped by ear bars to a stereotactic apparatus (Fig. 1). The dorsal surface of the right brain hemisphere of anaesthetized rats (i.p. injection of 5% sodium pentobarbital, 0.1 ml per 100 g of body weight) was exposed by a craniotomy; the dura was removed and immediately thereafter, for the course of the experiment, the exposed brain surface was covered with a mixture of mineral oil and petroleum jelly. Rectal temperature was maintained at 36.5–37°C by a servo-controlled heating pad. Supplementary i.p. injections of 0.05 ml 5% pentobarbital were given as necessary, and the mucous was periodically aspirated from the trachea throughout the experiment. The exposed surface of the right primary motor cortex was electrically stimulated (bipolar or monopolar) with silver-ball electrodes (diameter, 0.5 mm). For the specific stimulation of the hindlimb CS neurons (9–11) the electrodes were placed at the following P,L (P, posterior to bregma; L, lateral to the midline) coordinates: A, for bipolar stimulation, the rostral electrode at P = 0 to −1 mm, L = 1.5 to 2 mm and the caudal electrode at P = −4 to −5 mm, L = 1 to 2 mm; and B, for monopolar stimulation the single electrode at P = 0 to −1 mm, L = 1.5 to 2 mm and the reference, a brass rod electrode in the rectum. For the electrical stimulation, 5 pulse trains of biphasic current (500 Hz, 0.2 msec/phase) were generated at a frequency of 1 train/sec. EMG recording was performed with bipolar Teflon-coated and multistranded stainless steel wires (50 μm bare diameter) that were inserted into the individual exposed fore- and hindlimb muscles (12). The EMG signal was amplified and filtered (30 Hz to 3 kHz bandpass), and monitored and photographed from a Tetronix storage oscilloscope.

RESULTS

CS Evoked EMGs in Normal Rats. First, the experimental conditions and cortical areal coordinates were identified and defined under which CS-evoked EMG responses can be elicited in the hindlimb muscles. In normal intact rat (n = 4), bipolar stimulation of the cortical hindlimb area with currents

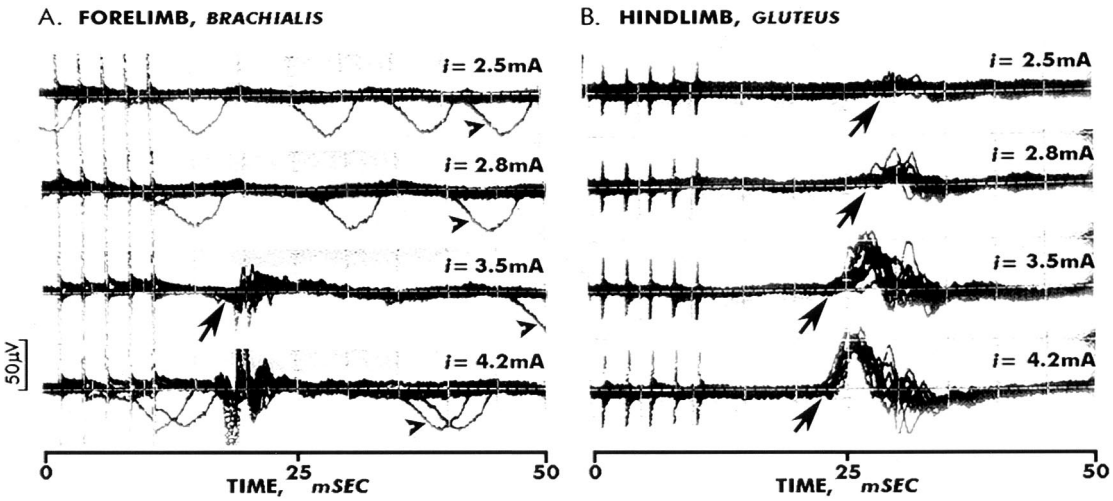

FIG. 2. Threshold and latencies of the CS-evoked EMG responses in the left forelimb and hindlimb muscles of a normal intact rat consequent to bipolar stimulation of the hindlimb area of the right motor cortex. Two composites of photographed traces of EMG responses that were recorded simultaneously in brachialis (A) and gluteus (B) and which are aligned from top-to-bottom according to the four stimulating current intensities (i). Each trace consists of ≈10 successive superimposed responses. The five deflections at the beginning of the trace are artifacts generated by the 5-pulse stimulus; their size grows with higher currents (B). Because the forelimb (A) is closer to the brain and heart, the artifact is larger than in the hindlimb's traces and the electrocardiogram appears in its traces as random downward deflections (arrowheads). The evoked responses in the fore- and hindlimb muscles have typical threshold latency values. Stimulating with 2.5 mA evoked a small response (arrow) in gluteus (B) at a latency of 28 msec; in contrast, there was no response in brachialis (A). The threshold response in brachialis (A) occurs at 3.5 mA with 17 msec latency (arrow). Increasing current intensity shortened the latency (arrows) (which reached in gluteus a value of 22 msec at 3.5 mA), recruited additional motor units, and increased the amplitude of the response (which peaked in gluteus to ≈50 μV). The response in brachialis was truncated for illustration purposes, its peak amplitude was over 200 μV.

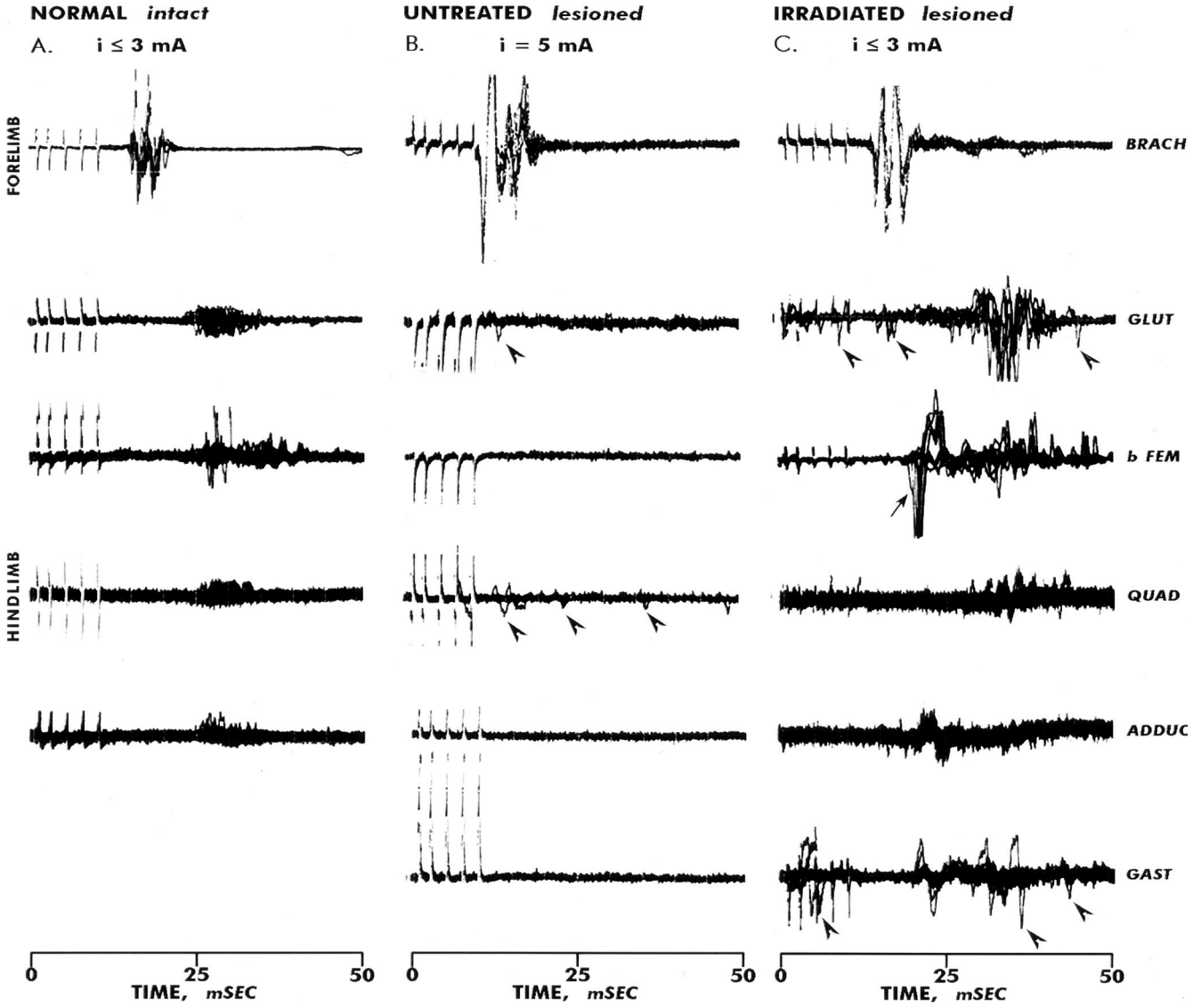

FIG. 3. CS-evoked EMG responses recorded in left limb muscles after bipolar stimulation of the hindlimb area of the right motor cortex of (*A*) normal intact rat, (*B*) untreated lesioned rat 65 days postinjury, and (*C*) irradiated lesioned rat 105 days postinjury. A composite of photographed traces of EMG responses are aligned from top-to-bottom according to the individual muscles recorded in: starting with the forelimb muscle (brachialis) and following with the hindlimb muscles (gluteus, biceps femoris, quadriceps, adductor, and gastrocnemius). Each trace consists of ≈10 successive superimposed responses that were evoked while the current intensity was increased, and the maximum intensities (*i*) applied are indicated for each of the rats; the five stimulus artifacts can be seen in most of the traces. In the three rats (*A–C*), evoked responses were recorded in the forelimb muscle at latencies in the range of 11–17 msec. No evoked responses were recorded in the hindlimb muscles of the lesioned unirradiated rat (*B*) (its cord is shown in Fig. 5 *a–d*). Evoked responses were recorded in all hindlimb muscles of the normal rat (*A*) and of the irradiated lesioned rat (*C*) (its cord is seen in Fig. 5 *Xa–Xd*), at latencies in the range of 22–27 and 21–28 msec, respectively. In the treated rat (*C*), in bicep femoris an additional evoked response was recorded at a latency of 17 msec (arrow); this appeared as a different component with a higher threshold current. Some of the hindlimb muscles of the lesioned rats (*B* and *C*) show spontaneous activity which is independent of the stimulus (recorded when no stimulation was given); this can be seen as random potentials (e.g., arrowheads) appearing without a fixed latency.

in the range of 1.8–3 mA evoked EMG responses in forelimb (brachialis) and hindlimb (gluteus, biceps femoris, quadriceps, adductor, and gastrocnemius) muscles (Figs. 2 and 3*A*). The latency times for the threshold responses in brachialis and in the hindlimb muscles (measured from the onset of the stimulus) were 17–19 and 27–30 msec (Fig. 2), respectively. Increasing the stimulating current from threshold level to 5 mA evoked responses in additional motor units while the latencies of the responses were shortened to 11–12 msec in brachialis (Fig. 3*B*) and to 18–22 msec in hindlimb muscles (Fig. 2*B*). The time interval between the latencies of the responses evoked by the same stimulus in forelimb and hindlimb muscles was in the range of 5–10 msec (e.g., Fig. 2). Based on these time interval values and the approximated distance of 70 mm between cord segments C6 and L4, the estimated values of the conduction velocity of the axons mediating the responses in the hindlimb muscles were deduced to be in the range of 7–14 m/sec. These values fit well with the measured antidromic conduction velocities in the rat CS tract, reported to be in the range of 5–19 m/sec (mean 11.4 ± 2.9 m/sec) (13). The properties of the evoked EMG responses were the same when using monopolar stimulation in the range of 0.75–1.25 mA. The differences between the latencies of the forelimb and hindlimb responses were 5–9 msec and the estimated conduction velocities were in the range of 7.8–14 m/sec.

Further, the experimental conditions under which EMG responses were elicited in discrete muscles were extremely sensitive to small changes in the placement of the stimulating

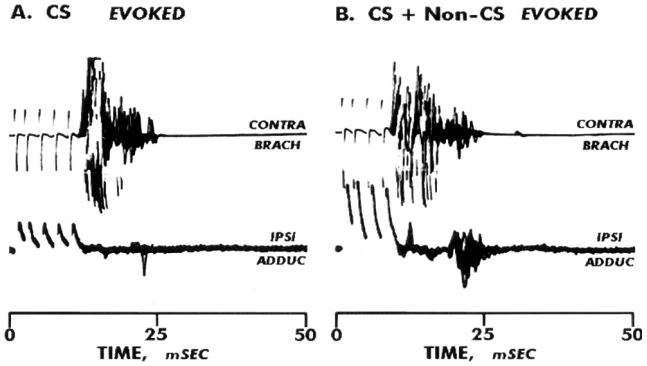

FIG. 4. Specific stimulation of the CS pathway and/or of a non-CS pathway. Evoked EMG responses recorded in a left forelimb muscle and in a right hindlimb muscle of a normal intact rat after monopolar stimulation of the right primary motor cortex. (*A*) Response evoked by 1.5 mA; under these conditions only the left muscle (brachialis) responds at a latency of 12 msec. (*B*) Responses evoked by a 2-mA stimulus (four pulses only). Under these conditions, the current spread to pathways other than the CS and responses were evoked also in the right muscle (adductor); these non-CS-evoked responses have latency times of 9 msec in brachialis, and 11 and 17 msec in the right adductor. It is assumed that the second response in adductor was evoked by a stimulus propagating via a combined pathway of the lateral cortico-reticulospinal tracts (14).

electrode in the anterior–posterior direction. For example, by moving the rostral electrode from 0 to −1 mm (with respect to bregma) at bipolar stimulating current of 1.8–2.5 mA, the evoked response in the forelimb muscle was lost (Fig. 2*A*) while it persisted in the hindlimb muscle (Fig. 2*B*). The stimulation evoked also discrete body/muscle movements that were exclusively unilateral, and no responses were recorded in the right hindlimb muscle (adductor) with either bipolar stimulation at 5 mA or with monopolar stimulation at current levels up to 1.4–1.5 mA (Fig. 4*A*).

In addition, areal and electrical stimulation conditions were identified under which non-CS-evoked EMG responses can be elicited. For example, increasing the current in monopolar stimulation to 2 mA evoked ipsilateral EMG responses—i.e., in the right hindlimb muscle (Fig. 4*B*). These responses had parameters different from those typical for the CS-evoked responses; they had shorter latency times of 6.5–8 and 8–10.5 msec in the forelimb and the hindlimb muscles, respectively, and a shorter interval in between the two latencies of 1–2.5 msec (Fig. 4*B*). The estimated values of conduction velocity of the axons mediating these responses (deduced as described above) are in the range of 28–70 m/sec, values typical for the reticulospinal tract that were reported to be in the range of 16–80 m/sec (mean = 37 m/sec) (15). Thus, we assume that these responses were evoked by the reticulospinal tract. These low-threshold contralateral and high-threshold ipsilateral evoked responses as obtained here by surface stimulation (Fig. 4) are similar to those obtained by intracortical microstimulation of the motor cortex in normal adult rat (16).

Response in Control Lesioned and Untreated Rats. Severance of the CS tract (Fig. 5 *a–c*) above the lumbar segments resulted in a complete loss of the CS control of the hindlimb muscle activity (Fig. 3*B*). No CS-evoked EMG responses—as defined for the normal intact rat—were recorded in hindlimb muscles of the rats with lesioned spinal cords (hemisection, n = 7; completely transected, n = 2), consequent to either bipolar stimulation (n = 7) at currents up to 5 mA (Fig. 3*B*) or monopolar stimulation (n = 2) at currents up to 1.5 mA. However, concurrently CS-evoked responses were recorded from the forelimb muscle (Fig. 3*B*) that is innervated by cervical motoneurons situated rostral to the cut. These lesioned and unirradiated rats were examined at 2, 20, 34, 40, 42, 65, 151, or 156 days after injury. In some of the rats with hemisectioned spinal cord non-CS-evoked responses—as defined for the normal intact rat (Fig. 4*B*)—were recorded in some of their hindlimb muscles. These responses were evoked presumably by the ipsilateral (right) reticulospinal axons (17–19), which were spared during the hemisection. No such responses were recorded in the rats with the completely transected cords.

Recovery of CS-Evoked EMGs in Irradiated Rats. In comparison with the lesioned untreated rats, we found that the severed CS tract in the rats with irradiated lesioned spinal cords (Fig. 5 *Xa–Xd*) regained some of its electrophysiologic control of the hindlimb muscles (Fig. 3*C*). CS-evoked EMG responses—as defined for the normal intact rat—were elicited (Fig. 3*C*), after stimulation of the cortical hindlimb area of the irradiated lesioned rats (hemisectioned, n = 6; completely transected, n = 3), in at least one of the hindlimb muscles in eight of the nine tested animals (Table 1). The EMG responses in the irradiated rats had properties similar to the CS-evoked responses in normal intact rats, in that they were evoked at the same or lower threshold (bipolar, 1.3–2.5 mA) and had similar latencies. In the treated rats, the measured time interval between the latencies of the evoked responses in the forelimb

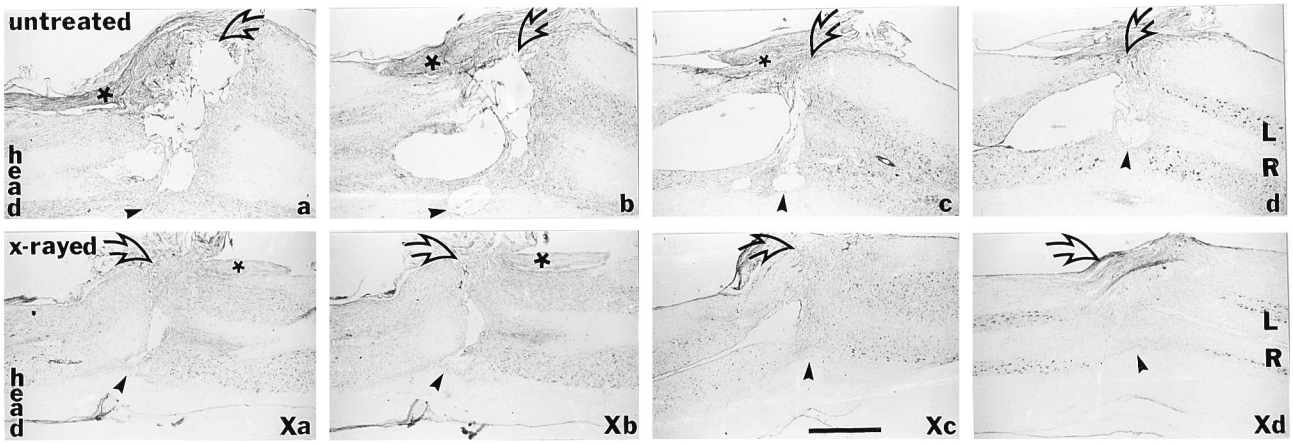

FIG. 5. The morphological features of the lesion site in two lesioned cords, unirradiated (*a–e*) and irradiated (*Xa–Xe*), obtained from the rats whose EMG recordings are shown in Fig. 3*B* and Fig. 3*C*, respectively. Serial reconstruction of the two cords are shown; each panel is a composite of thionin-stained horizontal sections taken from different regions along the dorsal–ventral direction. Indicated are the left (L) and the right (R) hemicords, the extent of incision traversing from left (clear arrow) past the midline and into the right hemicord (arrowhead), and the dorsal nerves (asterisks). Note in the untreated cord the cavitation and tissue degeneration throughout the entire volume surrounding the incision site. In the irradiated cord the incision disappeared and an almost complete structural continuity was established. (Bar = 1 mm.)

Table 1. Functional recovery of the severed left CS tract in irradiated hemisectioned and completely transected cords

Rat no.	Days Post injury	CS evoked EMG response in muscles						
		Left side					Right side	
		Glut.	Bic. fem.	Quad.	Add.	Gast.	Glut.	Add.
8a	105	+	−	−	−	−	ND	−
9a	101	+	−	+	+	−	ND	−
13a	105	+	+	+	+	+	ND	−
3a*	41	+	ND	+	+	ND	ND	+
4a*	46	+	−	−	+	+/−	ND	−
11a*	70	−	+	−	−	ND	ND	−
3b	130	+	−	+	−	−	ND	+
11b	143	−	+	+	+	−	+	−
12b	147	−	−	−	−	−	−	−

Summarized are the CS-evoked responses recorded in five left and two right hindlimb muscles in a total of nine irradiated rats. a, Hemisectioned; b, Completely transected; ND, not determined; Glut., gluteus; Bic. fem., biceps femoris; Quad., quadriceps; Add., adductor; Gast., gastrocnemius. *Monopolar stimulation.

and hindlimb muscle were in the range of 6–12 msec when the stimulation was either bipolar or monopolar at currents up to 5 mA and 1.25 mA, respectively. The estimated conduction velocities of the axons mediating these responses were in the range of 5.4–11.7 m/sec. It appears that some of the regenerated CS axons had slower conduction velocities than those of the normal intact CS tract as described above—i.e., 5.4 versus 7 m/sec. The decrease in conduction velocity suggests that some of the regenerated axons were not remyelinated (20).

In five of the nine irradiated lesioned rats, CS-evoked responses were recorded in three or more of the hindlimb muscles (Table 1). Most importantly, the degree of recovery of CS-evoked EMG responses appears to be related to the degree of structural recovery of the lesioned cord. The best recovery of control of muscle activity was observed (Fig. 3*C*) in the rat in which an almost complete structural continuity of the transected cord was obtained (Fig. 5 *Xa–Xd*). In this rat the regenerating CS axons had reached sacral cord segments establishing direct or indirect synaptic connection with motoneurons innervating the gastrocnemius. Finally, as established anatomically (5), upon regeneration the severed CS tract seems to loose its unilaterality. In several cases, primarily in the completely transected cords, some of the severed left CS axons also regrew into the right hemicord, establishing synaptic connectivity there and control of right hindlimb muscles (Table 1).

Functional Recovery in the Hindlimbs by X-Ray Therapy. The recovery in function of severed axons induced by the irradiation could be detected also visually. Irradiated ($n = 11$) and unirradiated ($n = 6$) rats that sustained a complete transection of their spinal cords were qualitative observed 4–5 months postinjury for the function and control of their hindlimbs when placed on a smooth metallic platform. Complete transection of the cord results in complete loss of function and control of the hindlimbs; the posterior body, distal to the cut, is paralyzed and lies flat on the surface (Fig. 6 *A–C*). In comparison, irradiation of the lesion site appears to elicit some functional recovery in the hindlimbs and in the body muscles distal to the lesion; some of the irradiated rats ($n = 6$) regained plantar foot contact and the ability to support weight and body posture (Fig. 6 *Ax–Cx*). This recovery of function correlates with the degree of restitution of structural continuity as determined histologically. It should be noted that none of the rats were exercised, and that in both groups there was a recovery within a few days postinjury of the reflex responses elicited, for example, by pinching of the skin distal to lesion.

DISCUSSION

The present study demonstrates that the anatomical recovery of the severed CS tract (5), made possible by the x-ray treatment, is accompanied by some electrophysiological recovery of its disrupted circuitry. That is, the regenerating CS axons establish connections, in remote cord regions distal to the lesion site, with neurons that control muscle activity. Our data are consistent with data obtained in a different CNS region (21); in that study, utilizing peripheral nerve grafts it was demonstrated that severed optic nerve fibers that regenerate along the graft and succeed in penetrating into the superior colliculus (CNS environment) also reestablish synaptic functional connectivity with target neurons there. Raisman (22), in a comparative study about synapse formation after injury in the adult peripheral and central neural tissues, demonstrated that the mechanisms of synapse formation and synapse matching are preserved in adult CNS. He also noted that the major difference in response to injury between the peripheral and the central neural tissues is that: "in the peripheral nervous site the originally cut axons can regenerate back to their former targets. [while in the CNS] . . . it seems most likely that the defect resides in an inability of the cut axons to regenerate across the site of injury in a manner necessary for them to reach the denervated target tissue." (22). In our study, the "defect" in lesioned spinal cord was corrected by a timed specific elimination of a group of reactive cells and

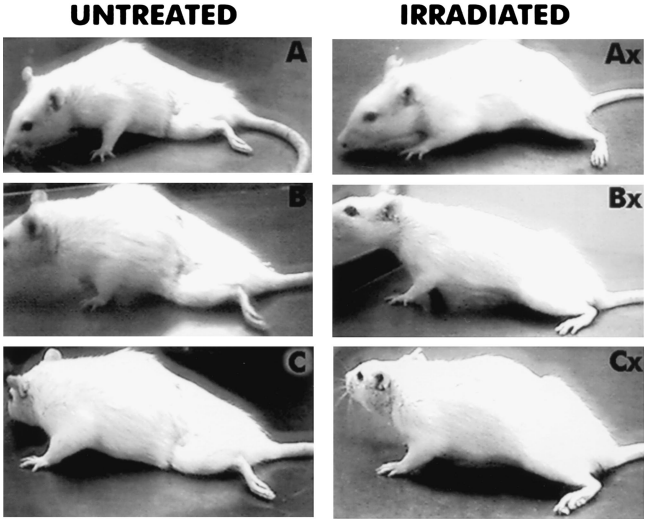

FIG. 6. Recovery of function of the hindlimbs. Photographs of two rats with completely transected spinal cords 4–5 months after injury. (*A–C*) Control, untreated rat. (*Ax–Cx*) Irradiated rat. The two rats are shown at identical views, focusing on their back distal to the lesion. Note in the irradiated rat the recovery in hindlimb posture and weight support—i.e., the position of the leg and the distance of the body, distal to the cut, from the surface on which the rat is standing.

the cut axons regenerated across the site of injury reaching denervated tissue forming synapses there, though not necessarily with their former target cells. Thus, it appears that the ability of the cut axons to cross the lesion site is related to the prevention of the degeneration and of the cavitation.

Irradiation seems to be a powerful tool for analyzing the sequelae of CNS injury (5, 6). It appears that it also may be developed into a therapeutic modality for facilitating functional recovery from injury. We can conclude from data presented here that prevention of tissue degeneration and the establishment of structural continuity is a sufficient requirement for the severed CS axonal tracts to reestablish synaptic connectivity and regain electrophysiologic control of neurons within the target field in the distal cord stump. We can infer from the recovery of function, such as recovery of body posture distal to the lesion site, that other disrupted circuitries had been reconnected. Thus, we propose that the first and essential step of a therapeutic protocol for the prevention of muscle paralysis—the reestablishment of synaptic connectivity—can be achieved by posttraumatic irradiation of the lesioned cord. As for reaching the final therapeutic goal of acquiring recovery of locomotion, this requires, in addition to the restitution of the disrupted individual circuitries, the restitution of the synaptic coordination between the individual circuitries that have been disrupted by the injury (see ref. 23). Manipulation and modulation of multiple circuitries (e.g., in the visual system), changing the cortical ocular dominance pattern can be achieved by training (e.g., eye patching) and/or by pharmacological treatment (24, 25). Thus, in addition to radiation therapy, a protocol for achieving behavioral motor recovery in adult mammals may require exercising, retraining, and/or pharmacological manipulations that affect synaptic remodeling and innervation patterns (see refs. 24–26).

This paper is dedicated to Miriam Salpeter and Mary Ellen Michel-Cheung, who examined our data with open mind and intellectual enthusiasm and infused encouragement during our effort to bring this research to light. The electrophysiological data, except for those reported in Fig. 2, were collected at The Rockefeller and Hahnemann Universities in the laboratories of Susan Schwartz-Giblin. We thank William Paul Hurlbut and Patricia Wade for their comments and help in the writing and editing of this article, and Philip Siekevitz for his unfailing help in publishing our studies.

1. Ramón y Cajal, S. (1928) *Degeneration and Regeneration of the Nervous System*, trans. May, R. M. (Oxford Univ. Press, London), Vol. 2, pp. 482–530.
2. Noble, L. J. & Wrathall, J. R. (1985) *Exp. Neurol.* **88,** 108–122.
3. Kakulas, B. A. (1987) *Paraplegia* **25,** 212–216.
4. Bresnahan, J. C. (1978) *J. Neurol. Sci.* **37,** 59–82.
5. Kalderon, N. & Fuks, Z. (1996) *Proc. Natl. Acad. Sci. USA* **93,** 11179–11184.
6. Kalderon, N., Alfieri, A. A. & Fuks, Z. (1990) *Proc. Natl. Acad. Sci. USA* **87,** 10058–10062.
7. Brown, L. T. (1971) *Exp. Brain Res.* **13,** 432–450.
8. Vahlsing, H. L. & Feringa, E. R. (1980) *Exp. Neurol.* **70,** 282–287.
9. Hall, R. D. & Lindholm, E. P. (1974) *Brain Res.* **66,** 23–38.
10. Zilles, K. & Wree, A. (1985) in *The Rat Nervous System*, ed. Paxinos, G. (Academic, Sidney, Australia), Vol. 1, pp. 375–415.
11. Donoghue, J. P. & Wise, S. P. (1982) *J. Comp. Neurol.* **212,** 76–88.
12. Cottingham, S. L., Femano, P. A. & Pfaff, D. W. (1987) *Exp. Neurol.* **97,** 704–724.
13. Mediratta, N. K. & Nicoll, A. R. (1983) *J. Physiol. (London)* **336,** 545–561.
14. Robbins, A., Schwartz-Giblin, S. & Pfaff, D. W. (1990) *Exp. Brain Res.* **80,** 463–474.
15. Fox, J. E. (1970) *Brain Res.* **23,** 35–40.
16. Kartje-Tillotson, G., Neafsey, E. J. & Castro, A. J. (1985) *Brain Res.* **332,** 103–111.
17. Waldron, H. A. & Gwyn, D. G. (1969) *J. Comp. Neurol.* **137,** 143–154.
18. Zemlan, F. P. & Pfaff, D. W. (1979) *Brain Res.* **174,** 161–166.
19. Martin, G. F., Vertes, R. P. & Waltzer, R. (1985) *Exp. Brain Res.* **58,** 154–162.
20. Waxman, S. G. (1977) *Arch. Neurol.* **34,** 585–589.
21. Keirstead, S. A., Rasminsky, M., Fukuda, Y., Carter, D. A., Aguayo, A. J. & Vidal-Sanz, M. (1989) *Science* **246,** 255–257.
22. Raisman, G. (1977) *Philos. Trans. R. Soc. London B* **278,** 349–359.
23. Sanes, J. N., Suner, S. & Donoghue, J. P. (1990) *Exp. Brain Res.* **79,** 479–491.
24. Simon, D. K., Prusky, G. T., O'Leary, D. D. M. & Constantine-Paton, M. (1992) *Proc. Natl. Acad. Sci. USA* **89,** 10593–10597.
25. Maffei, L., Berardi, N., Domenici, L., Parisi, V. & Pizzorusso, T. (1992) *J. Neurosci.* **12,** 4651–4662.
26. Barbeau, H. & Rossignol, S. (1994) *Curr. Opin. Neurol.* **7,** 517–524.